J|A|C|S
COMMUNICATIONS

Published on Web 12/15/2006

A Single-Molecule Magnet with a "Twist"

Constantinos J. Milios,[†] Alina Vinslava,[‡] Peter A. Wood,[†] Simon Parsons,[†] Wolfgang Wernsdorfer,[§] George Christou,[‡] Spyros P. Perlepes,[||] and Euan K. Brechin*,[†]

School of Chemistry, The University of Edinburgh, West Mains Road, Edinburgh EH9 3JJ, UK, Laboratoire Louis Néel-CNRS, 38042 Grenoble, Cedex 9, France, Department of Chemistry, University of Florida, Gainesville, Florida 32611-7200, and Department of Chemistry, University of Patras, 26504 Patras, Greece

Received September 21, 2006; E-mail: ebrechin@staffmail.ed.ac.uk

The origin of the ferromagnetic exchange in a recently reported oxo-centered triangular Mn(III) single-molecule magnet (SMM) based on oximato ligands is fascinating since the exchange in all other complexes containing the $[Mn^{III}_3O]^{7+}$ core, including the well-known "basic carboxylates" of general formula $[Mn^{III}_3O(O_2CR)_6L_3]^+$ (R = Me, Et; L = py, MeCN, etc.), is antiferromagnetic.[1] We speculate that a structural distortion in the core of the molecule caused primarily by the "twisting" of the oximato ligands (with regard to the Mn^{III}_3 plane) is responsible. In order to test this hypothesis we have made a family of novel ligands based on salicylaldoxime ($saoH_2$) in which the oximate carbon atom has been derivatized to possess the "bulky" Me (Me-$saoH_2$), Et (Et-$saoH_2$), and Ph (Ph-$saoH_2$) groups, and synthesized analogues of the known hexanuclear SMM $[Mn^{III}_6O_2(sao)_6(O_2CPh)_2(EtOH)_4]$ (**1**).[2] Complex **1**, obtained upon the reaction of $Mn(O_2CPh)_2{\cdot}2H_2O$ with $saoH_2$ in EtOH (Figure S1) contains a nonplanar $[Mn^{III}_6(\mu_3\text{-}O)_2(\mu\text{-}OR)_2]^{12+}$ unit of two off-set, stacked $[Mn^{III}_3(\mu_3\text{-}O)]^{7+}$ triangular subunits linked by two central oximato oxygens, with the remaining four sao^{2-} ligands bridging in a near-planar $\eta^1{:}\eta^1{:}\eta^1{:}\mu$-fashion along the edges of the $[Mn^{III}_3(\mu_3\text{-}O)]^{7+}$ triangles. The four "central" metals (Mn1, Mn3) are six-coordinate and in distorted octahedral geometries, while the outermost Mn ions (Mn2) have square pyramidal geometries with an additional axial contact of ~3.5 Å to a phenolato oxygen. The coordination geometry of the metal ions is completed by a combination of terminal alcohols and μ-carboxylate groups. **1** displays an $S = 4$ spin ground state as a result of ferromagnetic exchange between the two antiferromagnetically coupled Mn^{III}_3 triangles.[2]

The idea was to investigate whether the additional steric bulk of the derivatized oximates would enforce structural distortions similar to those seen in the ferromagnetic Mn_3 triangle[1] and the recently obtained ferromagnetic $[Mn^{III}_4(Me\text{-}sao)_4(Me\text{-}saoH)_4]$ "cube",[3] and thus switch the magnetic behavior from antiferromagnetic to ferromagnetic. Complex $[Mn^{III}_6O_2(Et\text{-}sao)_6(O_2CPh)_2(EtOH)_4(H_2O)_2]{\cdot}$ 2EtOH (**2**·2EtOH) which contains the ethyl-derivatized $saoH_2$ (Et-$saoH_2$) does indeed display ferromagnetic exchange ($S = 12$ ground state). Here we discuss its structure and magnetic properties. Complex **2** also crystallizes in the triclinic space group $P\bar{1}$ and its structure (Figure 1) is analogous to that of **1**.[4] However, the increased steric bulk of the Et-sao^{2-} ligands causes a shortening of the phenolato oxygen (O71)−square pyramidal Mn (Mn3) distance (~2.5 Å) and severe twisting of the Mn−N−O−Mn moieties within each Mn_3 subunit (Figure 1). This is evidenced by the average Mn−N−O−Mn torsion angle, which in **1** is $\alpha_v = 17.5°$ compared to $\alpha_v = 36.5°$ for **2**. This also results in a change in the coordination of the carboxylates: from μ-bridging to terminal, with the "vacant" site now occupied by an additional solvent (alcohol) molecule.

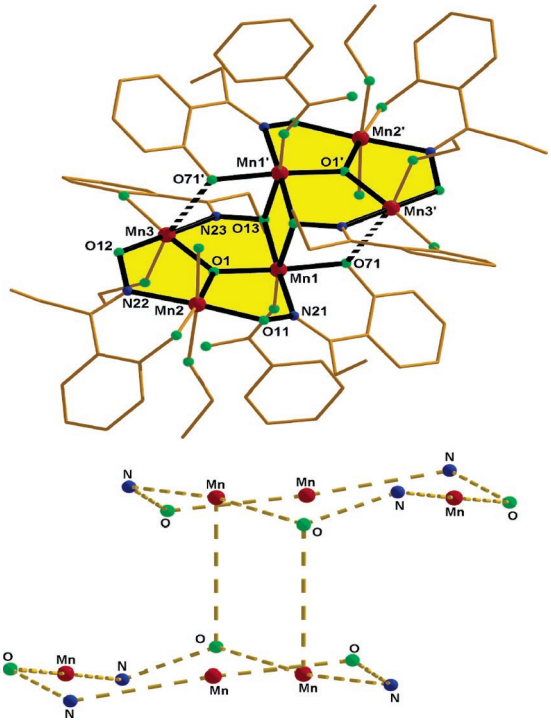

Figure 1. The molecular structure of complex **2**, highlighting its core (top); the "twisted" Mn−N−O−Mn arrangement of the Etsao^{2-} ligands in **2** (bottom).

Variable-temperature dc magnetic susceptibility data were collected on **2** in the temperature range 5−300 K in an applied field of 0.1 T (Figure S2). The room temperature $\chi_M T$ value of 19.24 cm^3 K mol^{-1} is slightly above that expected for six noninteracting Mn^{III} ions (18 cm^3 K mol^{-1}). Upon cooling the value of $\chi_M T$ increases gradually to 23.72 cm^3 K mol^{-1} at ~70 K, below which it increases rapidly to a maximum value of 69.57 cm^3 K mol^{-1} at 6.5 K, before decreasing slightly to 69.36 cm^3 K mol^{-1} at 5 K. This behavior is indicative of ferromagnetic exchange between the metal centers with the low-temperature maximum suggesting an $S = 12$ ground state. In order to confirm the ground state of the molecule, magnetization data were collected in the ranges 0.5−7 T and 1.8−7 K, and these are plotted as reduced magnetization ($M/N\mu_B$) versus H/T in Figure 2. The data were fit by a matrix diagonalization method to a model that assumes only the ground state is populated, includes axial zero-field splitting ($D\hat{S}_z^2$) and the Zeeman interaction, and carries out a full powder average. The corresponding Hamiltonian is given by eq 1,

[†] University of Edinburgh.
[‡] University of Florida.
[§] Laboratoire Louis Néel-CNRS.
[||] University of Patras.

10.1021/ja0666755 CCC: $37.00

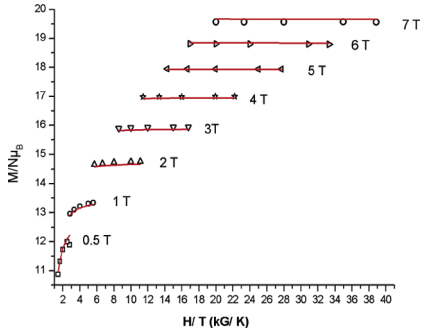

Figure 2. Plot of reduced magnetization ($M/N\mu_B$) versus H/T for **2** in the field and temperature ranges 0.5−7 T and 1.8−7 K. The solid lines correspond to the fit of the data.

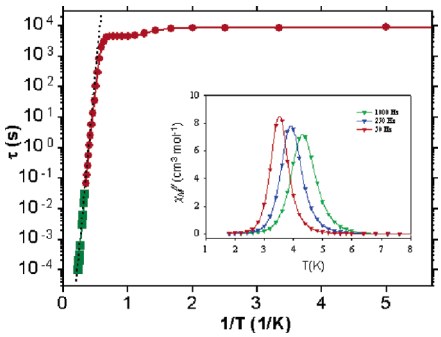

Figure 3. Out-of-phase (χ_M'') ac susceptibility measurements in the 1.8−8 K and 50−1000 Hz ranges (insert); Arrhenius plot using ac (green) and dc (red) data. The dashed line is the fit of the thermally activated region to eq 2.

$$\hat{H} = D\hat{S}_z^2 + g\mu_B\mu_0\hat{S}\cdot H \qquad (1)$$

where D is the axial anisotropy, μ_B is the Bohr magneton, μ_0 is the vacuum permeability, $\hat{S}_z$ is the easy-axis spin operator, and H is the applied field. The best fit gave $S = 12$, $g = 1.99$ and $D = -0.43$ cm^{-1}.

Ac susceptibility measurements were performed in the 1.8−16 K range under a 3.5 G ac field oscillating at 50−1000 Hz. The value of the in-phase ($\chi_M'T$) signal (Figure S3) increases with decreasing temperature to ∼6 K where it then plateaus at ∼4 K before displaying a frequency-dependent decrease below this temperature. This is indicative of the presence of excited states of smaller S values relatively close to the ground state. Extrapolation of the in-phase ($\chi_M'T$) signal to 0 K from the plateau region gives a value of ∼74 cm^3 K mol^{-1} indicative of an $S = 12$ ground state, in agreement with the dc data (Figure S3). Fully visible, frequency-dependent out-of-phase (χ_M'') ac susceptibility signals are seen below ∼6 K with the peak at 1000 Hz occurring at ∼4.5 K (Figure 3).

Single-crystal hysteresis loop and relaxation measurements were performed on **2** using a micro-SQUID setup.[5] Hysteresis loops were observed whose coercivity was strongly temperature (Figure 4) and sweep-rate (Figure S4) dependent, with a blocking temperature of ∼3.5 K. Relaxation data determined from a combination of single-crystal dc and powder ac measurements were fitted to the Arrhenius relationship (eq 2, Figure 3),

$$\tau = \tau_0 \exp(U_{eff}/kT) \qquad (2)$$

where U_{eff} is the effective relaxation barrier, τ is the relaxation time, and k is the Boltzmann constant, giving $U_{eff} = 53.1$ K and $\tau_0 = 8 \times 10^{-10}$ s. The theoretical upper limit of $U = S^2|D| = 88.5$ K is strongly reduced by the presence of low-lying excited states as

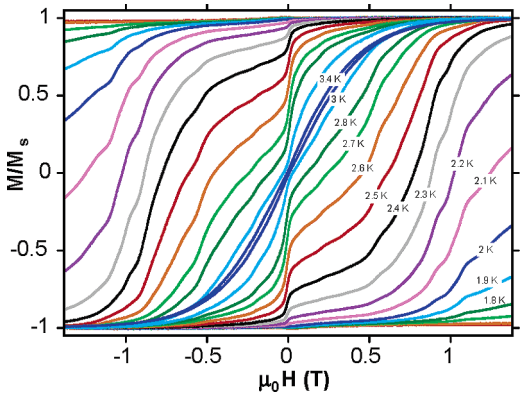

Figure 4. Magnetization versus field hysteresis loops for a single crystal of **2** at the indicated temperatures in a field sweep rate of 0.14 T s^{-1}. M is normalized to its saturation value.

evidenced by the fine structure in the hysteresis loops which are indicative of tunneling between excited-state multiplets. Detailed analyses of these will appear in a full paper.

In conclusion, the deliberate structural distortion of a Mn_6 compound via the use of a bulky salicylaldoxime derivative switches the intra-triangular magnetic exchange from antiferromagnetic to ferromagnetic resulting in an $S = 12$ ground state and an anisotropy barrier (U_{eff}) approaching that of the Mn_{12} family.[7,8] The combined results thus suggest that the intelligent use of ligands that can cause targeted distortions to the core structures of Mn_6 (and other) clusters may prove to be a viable means to raise the blocking temperatures of SMMs to record values.

Acknowledgment. This work was supported by the Leverhulme Trust and EPSRC (UK), the NSF (U.S.A.), and PYTHAGORAS I (Greece).

Supporting Information Available: Crystallographic details in CIF format; synthetic procedures: and magnetism data. This material is available free of charge via the Internet at http://pubs.acs.org.

References

(1) Stamatatos, T. C.; Foguet-Albiol, D.; Stoumpos, C. C.; Raptopoulou, C. P.; Terzis, A.; Wernsdorfer, W.; Perlepes, S. P.; Christou, G. *J. Am. Chem. Soc.* **2005**, *127*, 15380.

(2) Milios, C. J.; Raptopoulou, C. P.; Terzis, A.; Lloret, F.; Vicente, R.; Perlepes, S. P.; Escuer, A. *Angew. Chem., Int. Ed.* **2003**, *43*, 210.

(3) Milios, C. J.; Prescimone, A.; Mishra, A.; Parsons, S.; Wernsdorfer, W.; Christou, G.; Perlepes, S. P.; Brechin, E. K. *Chem. Commun.* **2006**. http://dx.doi.org/10.1039/b611174b.

(4) Anal. Calcd (found) for dried **2** (solvent free): C 50.62 (50.78), H 5.14 (5.01), N 4.66 (4.51). Crystal data for **1**·2CH_3CH_2OH: $C_{80}H_{104}Mn_6N_6O_{26}$, FW = 1895.30 g mol^{-1}, T = 150 K, Triclinic $P\bar{1}$, a = 12.4947(9) Å, b = 13.2846(9) Å, c = 14.5047(11) Å, α = 71.488(4)°, β = 82.305(4)°, γ = 68.687(4)°, V = 2126.4(3) Å^3, d_{calcd} = 1.480 g cm^{-3}, independent refelections 11741 [R(int) = 0.034], data 8011, parameters 547, final R1 = 0.0339 for 8011 reflections with $F > 4\sigma(F)$. Conventional R [$F > 4\sigma(F)$], R1 = 0.0339 [8011 data].

(5) Wernsdorfer, W. *Adv. Chem. Phys.* **2001**, *118*, 99.

(6) For reviews see: (a) Christou, G.; Gatteschi, D.; Hendrickson, D. N.; Sessoli, R. *MRS Bull.* **2000**, *25*, 66. (b) Gatteschi, D.; Sessoli, R. *Angew. Chem., Int. Ed.* **2003**, *42*, 268. (c) Aromí, G.; Brechin, E. K. *Struct. Bonding* **2006**, *122*, 1. (d) Bircher, R.; Chabousant, G.; Dobe, C.; Güdel, H. U.; Ochsenbein, S. T.; Sieber, A.; Waldmann, O. *Adv. Funct. Mater.* **2006**, *16*, 209.

(7) (a) Caneschi, A.; Gatteschi, D.; Sessoli, R.; Barra, A. L.; Brunnel, L. C.; Guillot, M. *J. Am. Chem. Soc.* **1991**, *113*, 5873. (b) Sessoli, R.; Tsai, H. L.; Schake, A. R.; Wang, S. Y.; Vincent, J. B.; Folting, K.; Gatteschi, D.; Christou, G.; Hendrickson, D. N. *J. Am. Chem. Soc.* **1993**, *115*, 1804. (c) Sessoli, R.; Gatteschi, D.; Caneschi, A.; Novak, M. A. *Nature* **1993**, *365*, 141.

(8) Chakov, N. E.; Lee, S.-C.; Harter, A. G.; Kuhns, P. L.; Reyes, A. P.; Hill, S. O.; Dalal, N. S.; Wernsdorfer, W.; Abboud, K.; Christou, G. *J. Am. Chem. Soc.* **2006**, *128*, 6975.

JA0666755